AIAA 80-0059R

# Uncontrolled Dynamics of the Skylab Vehicle

H.J. Buchanan,* M.S. Hopkins,† and Z.J. Galaboff†
*NASA Marshall Space Flight Center, Huntsville, Ala.*

**In the four years the Skylab space station was uncontrolled, it moved from its stable gravity gradient orientation, through large angle motion and high spin rates, until control was re-established in May 1978. An understanding of the type of rotational motion was important for both lifetime predictions and regaining control. This paper describes the dynamic behavior of the Skylab during these transitions from both an analytical approach and the results obtained by numerically integrating the equations of motion. Flight data obtained in the spring of 1978 are presented which support the analytical and simulation results.**

## Introduction

THE Skylab vehicle was one of the largest man-made structures placed in orbit to date. When the final mission was completed in 1974, the on-board systems were used to maneuver the vehicle to a gravity gradient equilibrium attitude and were then shut down. Parked in this storage attitude, the vehicle was left undisturbed until March 1978, when contact was re-established and the control systems reactivated. During the intervening four years, the vehicle was subjected to subtle environmental torques which caused the vehicle to gradually progress from its initial stable state to a very dynamic condition just prior to the resumption of control. This paper will deal with the dynamics of this process including the analyses and simulations which were made to explain the motion and enable the planning of the reactivation process. This was a very interesting technical problem in its own right and similar ones may be found in the future.

## Configuration

Figure 1 shows the basic Skylab vehicle without an Apollo Command Service Module docked to it. This was the storage configuration and the one of interest in this case. Note that the vehicle has only a single solar array on the Orbital Workshop (OWS) instead of the pair originally intended. The missing array was torn off during launch and the resulting asymmetry had some important effects on vehicle motion which will be discussed later. Also, note that two body-fixed axis systems are portrayed. The $X_B$, $Y_B$, $Z_B$ is a geometric system located at the center of the mass. In many cases dynamic motion is more easily explained in terms of a principal axis system, $X_p$, $Y_p$, $Z_p$, with its origin at the center of mass and oriented so that the product of inertia terms vanish from the inertia matrix. Table 1 presents the mass and inertia data used in this study.[1]

### Original Attitude

The vehicle was originally positioned with its $X_p$ axis along the radius vector from the Earth's center and with the $Z_p$ axis pointing backward along the orbital path. This would be a stable equilibrium orientation if gravity gradient torques only were considered. Figure 2 depicts this orientation and also introduces the orbital coordinate frame which will be referred to from time to time. Confirmation of the accuracy of the final maneuver was not possible, but was thought to be ±5 deg. The vehicle's motion originally then would have consisted of some small amplitude oscillations about the local vertical. The vehicle's orbit was very nearly circular with an initial altitude of 435 km (235 n.mi.). At the time of reactivation this had decayed to approximately 398 km (215 n.mi.). The orbital inclination was 50 deg and the rate of orbit plane regression was approximately 5 deg/day.

### Current Interest

Decay of the Skylab orbit had been monitored on a routine basis, but in 1977 it became apparent that increased solar activity was affecting the atmospheric density and causing a more rapid decay. Concern over this prompted a more detailed look at aerodynamic drag which is, of course, dependent on attitude. It was soon recognized that the gravity gradient attitude had a relatively high drag associated with it and that by changing to a lower drag attitude the vehicle's orbital lifetime could be increased. Since a scheme for reboosting or deorbiting Skylab using a small propulsion unit brought up on an early Space Shuttle mission was being considered, an increase in orbital lifetime was very attractive. This increased interest prompted additional ground-based observations of the vehicle's attitude. Routine observations over the previous several years had generally confirmed that the original attitude had been preserved. In late 1977, similar observations seemed to indicate that the vehicle's attitude and motion were changing. Thus, one of the first tasks was to understand what was taking place and why. This had to be done before much credence could be given to future predictions of vehicle motion over the next several months.

## Related Dynamic Analyses

One approach to a problem of this type is to compute all the pertinent external torques acting on the vehicle and numerically integrate the equations of motion to obtain time histories of the vehicle motion. While this has the advantage of providing accurate results with few if any approximations, it generally makes the physics of the problem difficult to understand and explain. A better approach and the one used in this analysis draws upon simplified theoretical work to explain the nature of the motion in certain regimes. The numerical approach is then used to substantiate these conclusions and to combine the various effects. Theory and numerical results can be checked against each other at every stage and this greatly enhances confidence in the results. The major advantage, however, is in the explanation and interpretation of results. This is especially important in a problem of this type where much of the observed data seemed to contradict some elementary dynamic concepts. For example, data showed the vehicle had left the gravity gradient equilibrium orientation where it had stayed for over three years. Instead, the vehicle seemed to be oriented with the long axis perpendicular to the orbit plane (an unstable gravity

Presented as Paper 80-0059 at the AIAA 18th Aerospace Sciences Meeting, Pasadena, Calif., Jan. 14-16, 1980; submitted Jan. 17, 1980. 

*Chief, Dynamics and Trajectory Analysis Branch, Systems Dynamics Laboratory. Member AIAA.

†Aerospace Engineer, Dynamics and Trajectory Analysis Branch, Systems Dynamics Laboratory.

**Table 1 Skylab mass properties**

Principal moments of inertia

| | |
|---|---|
| $I_{xp} = 0.759 \times 10^6$ kg-m$^2$ | $(0.562 \times 10^6$ slug-ft$^2)$ |
| $I_{yp} = 3.896 \times 10^6$ kg-m$^2$ | $(2.8737 \times 10^6$ slug-ft$^2)$ |
| $I_{zp} = 3.823 \times 10^6$ kg-m$^2$ | $(2.8196 \times 10^6$ slug-ft$^2)$ |

Direction cosine matrix body to principal axes

$$[A]_{PB} = \begin{bmatrix} 0.9842 & 0.0210 & 0.1760 \\ 0.0162 & 0.9781 & -0.2073 \\ -0.1765 & 0.2069 & 0.9623 \end{bmatrix}$$

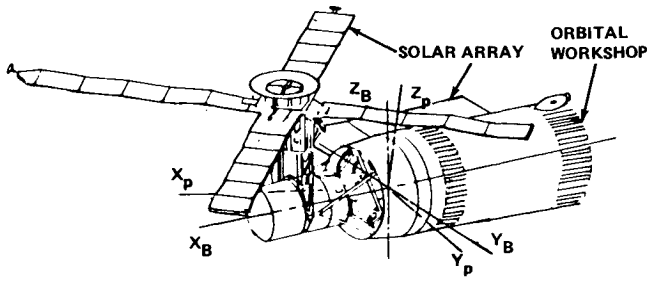


**Fig. 1 Skylab vehicle.**

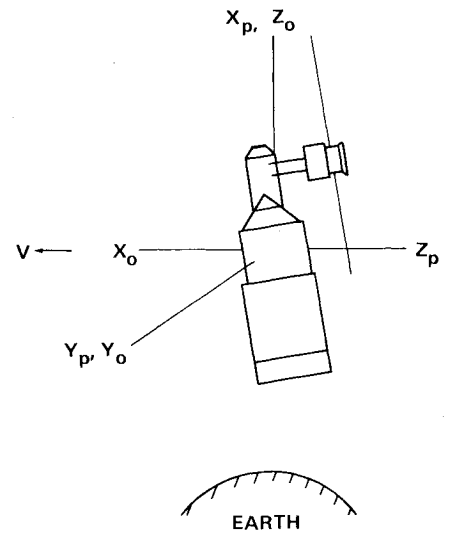


**Fig. 2 Orbital coordinate system and original Skylab attitude.**

gradient orientation). Also, the vehicle had developed a relatively rapid spin rate about the long axis and this gave every indication of accelerating. Since spin about this axis is generally unstable in the presence of energy dissipation (usually found in real systems) the development and persistence of this motion was puzzling.

Skylab's motion after it was parked in 1974 probably built up in stages. The exact time of transition between stages may never be known because the observations were made infrequently. It is known, however, that for many months it remained in its original gravity gradient orientation. In 1977, data showed the vehicle out of the gravity gradient equilibrium position and rotating through large angles. While some singular event, such as a meteoroid strike, a gas bottle leak, etc., could have been responsible, this seems unlikely since the status of the on-board systems did not support such an occurrence. Interestingly enough, there are other less dramatic explanations for what took place. A number of papers have been published dealing with the instability produced when a gravity gradient stabilized body is subjected to a torque which forces it slightly away from the true gravity gradient equilibrium position (i.e., axis of minimum inertia aligned with the radius vector and axis of maximum inertia aligned with the perpendicular to the orbit plane). This is sometimes called the "Garber Instability" after the author of the original paper.[2] It was shown by both Nurre[3] and Sperling[4] that in the original Skylab configuration (i.e., two OWS solar arrays) aerodynamic forces could produce the necessary perturbation, subjecting the vehicle to this instability. Both of the last two investigators were working with mass properties associated with the original Skylab configuration (i.e., two OWS arrays). An effort was therefore made to assess the effect of the absence of one solar panel on the aerodynamic torque disturbance and hence on the possible equilibria and stability of the Skylab.

Nurre and Sperling used Fourier Series to represent the aerodynamic forces and torques, taking advantage of symmetries, simplifications and various invariance conditions to achieve a reduction in the number of terms used. For our study such reductions were not always possible because the actual Skylab configuration did not exhibit these symmetries. Notwithstanding these conditions, the study basically paralleled the work of Sperling.[4] An attempt to do a complete search for equilibria for a given altitude and density combination was too costly and prohibitive by computer time requirements. However, from our large simulation, equilibrium orientations were obtained. A linearized infinitesimal analysis was then used to study the stability of the equilibrium orientations. An examination of the coefficients of the sixth degree characteristic polynomial of our system revealed that the coefficient of the fifth power was identically equal to zero. Since this coefficient is the sum of the roots of the characteristic polynomial, not all roots can have negative real parts. These results agree with Sperling's conclusion about the stability of the Skylab. An indication of the Skylab instability as a function of altitude is shown in a comparison of the logarithm of the amplitude over one orbit (logarithmic increment). The approximate logarithmic increments are $2.27 \times 10^{-3}$ and $2.60 \times 10^{-2}$ for altitudes of 435 km (235 n.mi.) and 278 km (150 n.mi.), respectively. It was also found that the roots were very sensitive to relatively small displacements from the equilibrium positions, thus tending to confirm the highly nonlinear nature of our problem.

With the weak instability indicated by these small logarithmic increments, a very small amount of energy dissipation (damping) could stabilize the vehicle. However, as the density increases (due to altitude decay or solar activity), the required damping to maintain stability would have to increase. On a vehicle like Skylab, energy dissipation is probably small in relative terms and could not be increased. An assessment to determine how much damping was available and the source of such damping was made when the first indications were received that the Skylab had left the gravity gradient attitude. Calculating backwards from the observed density, it appears that the system damping available should have been on the order of 0.01% of critical. The sources of damping considered were: 1) external damping as a result of interaction with the Earth's atmosphere and magnetic field (these were assessed and found to be below the required value); and 2) internal damping which would result from structural vibrations and the relative motion of internal parts. Once a structure is excited, structural damping values on the order of 0.5%[5] have been observed. In this case, however, the frequency of the gravity gradient motion is very low (only about 1.5 cycles per orbit). The lowest flexible body mode has a frequency approximately 1000 times greater[5] and would, thus, be very difficult to excite. Internal motion of large quantities of material inside the vehicle was difficult to justify. Liquids were thought to still be restrained by bladders and most equipment was secured in some fashion. Above all, the very low rates and acceleration levels being observed offered no plausible mechanism for exciting the material. It

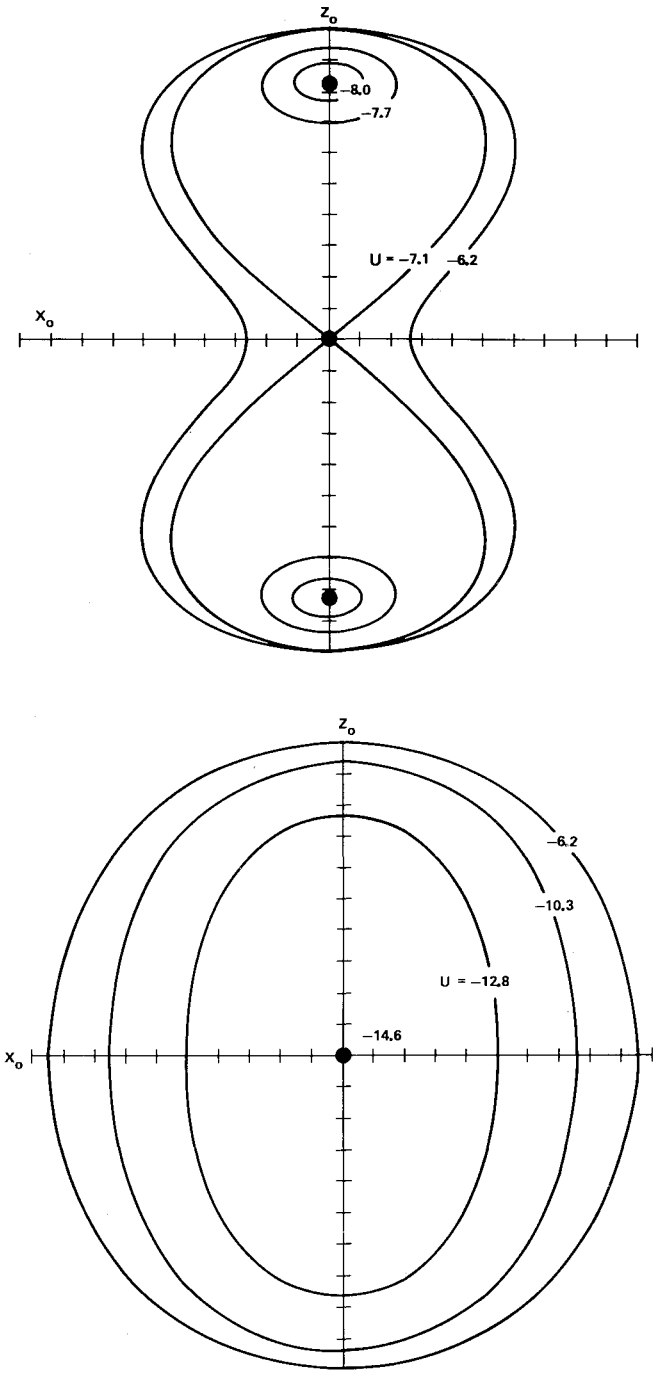


**Fig. 3 Dynamic potential contours viewed in the orbital frame at spin rate of a) 0.5 deg/s and b) 1.1 deg/s.**

would then appear that the very small damping value backed out of the stability analysis is consistent with that required to have maintained the Skylab in a stabilized gravity gradient attitude prior to the fall of 1977.

In view of these findings, it is our conclusion that 1) the system damping for the vehicle in the gravity gradient attitude was very small (i.e., on the order of 0.01% of critical) and 2) the vehicle left its gravity gradient orientation when the increase in atmospheric density strengthened the Garber effect until the small damping present was overwhelmed and the system became unstable.

Given this instability it was inevitable that large amplitude motion would build up. When this happened, another relatively small aerodynamic effect began to be felt. Because of the asymmetric OWS solar array configuration of this vehicle, the aerodynamic moments were unbalanced producing a tendency to spin up about the longitudinal axis. That is, if the vehicle were rotated slowly about the $x$ axis and the aerodynamic roll moment recorded, the integral over one complete revolution would not be zero. This effect is analogous to the aerodynamic effect which causes an anemometer to spin. Once started, rotation about this axis slowly accelerates. This effect was suspected after examination of the aerodynamic data[6] and was confirmed when these data were input to a dynamic simulation. At this point the puzzle as to why the vehicle had left its gravity gradient attitude and begun to spin had been largely answered. For a better understanding of the motion of the vehicle's spin axis in the orbital coordinate frame, it was decided to consult some of the analytical work on spinning satellites published during the past 20 years.

Because the moments of inertia about the $y$ and $z$ principal axes are nearly the same (Table 1), the problem closely resembles the classic body of revolution spinning about its axis of symmetry. The case of a symmetrical rigid body in a circular orbit has been considered by a number of authors and some of these results were very helpful in understanding both the observed vehicle motion and the computer simulation results. Pringle[7] formulated the problem in terms of a dynamic potential function, $U$, which he derived from the Hamiltonian. With the potential function he was then able to determine equilibrium orientations where a static balance existed between gyroscopic and gravitational torques. The stability of these equilibria was then examined and closed contours of the potential function used to illustrate the types of vehicle motion possible as a function of spin rate and inertia ratio. For a symmetric vehicle with the Skylab inertia ratio, contours of the potential function are shown in Fig. 3 for two spin rates over the range observed. These contours are plotted on the surface of a sphere with the viewer looking down the orbit normal. The filled circles represent stable equilibria and the contour lines can be interpreted as bounds on the motion of the spin axis. That is, if the spin axis is initially placed within a closed contour surrounding a stable point it will not cross that contour although its path will not necessarily parallel it. Note that for no spin, equilibrium is found with the axis of symmetry along the radius vector. As the spin rate increases, the equilibria move out of the orbital plane until at approximately 1 deg/s they combine into a single, stable orientation with the spin axis perpendicular to the plane.

It was found that this description was consistent with the results obtained from integrating the equations of motion. Equilibrium orientations were found where predicted and the closed contours were not violated. To determine the effects of the mass asymmetry, aerodynamic torques, and orbital regression, these were incorporated into the simulation individually and the resulting changes noted. By and large, these were found to be second order influences, but they were retained in the simulation for completeness. Actually, these effects have also been treated analytically in previous works, but not in a single analysis. Meirovitch[8] extended Pringle's work to include the effect of simple aerodynamic torques. In the cases he treated, this produced a small shift in the equilibrium point and a distortion in the contour lines. It was possible to confirm this qualitatively in our simulation, but because of the more complex aerodynamics a quantitative check could not be made. Several investigators (Cochran,[9] Pringle,[10] and others) have examined the effect of orbital regression on long-term vehicle motion. Briefly put, for spin rates below a critical value, the vehicle will precess and follow the orbital plane. If the rate is too fast, the body will try to remain inertially fixed and will not follow the movement of the orbital plane. In the case of Skylab, the rates were low and the motion did follow the orbital plane.

These analyses as well as work presented in Refs. 11-14 helped establish confidence in the numerical solutions obtained from the simulation program and provided a guide in

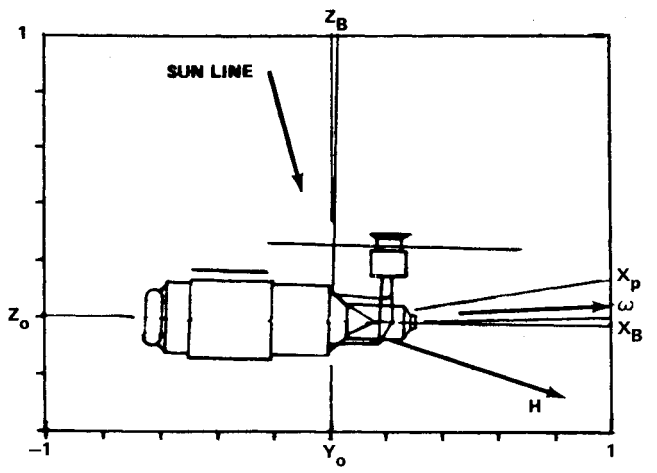


Fig. 4 Initial vehicle attitude for simulation results.

evaluating the contributions of the various effects. Without such a framework, this task would have been much more difficult.

## Simulation Description

The uncontrolled motion of the Skylab while in orbit was simulated using a six-degree-of-freedom (6 DOF) digital program on the Honeywell CP-V system. The equations of motion for a small rigid body in orbit about the Earth have been published in numerous documents and will not be restated here. If the reader is interested he is referred to Ref. 4 for a typical example. The rigid-body program utilizes an oblate rotating Earth model and includes the effects of perturbing torques due to gravity gradient and aerodynamic forces. Quaternions were used to represent the attitude of the uncontrolled vehicle and a variable step size, five-pass Runge-Kutta integration scheme was used. Using this scheme, the Skylab motion could be simulated for approximately a month's time without appreciable integration roundoff errors.

The Jacchia 1970-3 atmosphere model and the predicted solar and geomagnetic activities data used to determine density profiles were provided by Space Sciences Laboratory, MSFC. These predicted data were based on the smoothed 13-month mean values and were updated monthly. A detailed description of the model is given in Ref. 15.

The Skylab in-orbit aerodynamic data are given in Ref. 6. Force and moment coefficients for each of the three body axes are given as a function of angle of attack and aerodynamic roll angle. The data cover all possible orientations of the Skylab and were used in the simulation in table lookup form.

In the following section results obtained from this simulation are presented and compared with data obtained from vehicle telemetry.

## Comparison of Telemetered Data and Simulation Results

After contact was established with the vehicle in March, data were available from the on-board sensors and this was examined for clues to the vehicle's behavior. The two major sources of data were the vehicle's rate gyro system and the solar array system; however, each of these had certain limitations. The rate gyros provided an accurate source of rate information, but were scaled so that only rates below 1 deg/s could be measured. As the $x$ axis rate was greater than this, only the sign was available for this axis. A fairly accurate measurement of the roll rate magnitude could be obtained by timing the light/dark cycle observed in the solar array output, but the axis of rotation could not be determined accurately. The strength of the output from the solar arrays gave some indication of the sun incidence angle on the solar arrays.

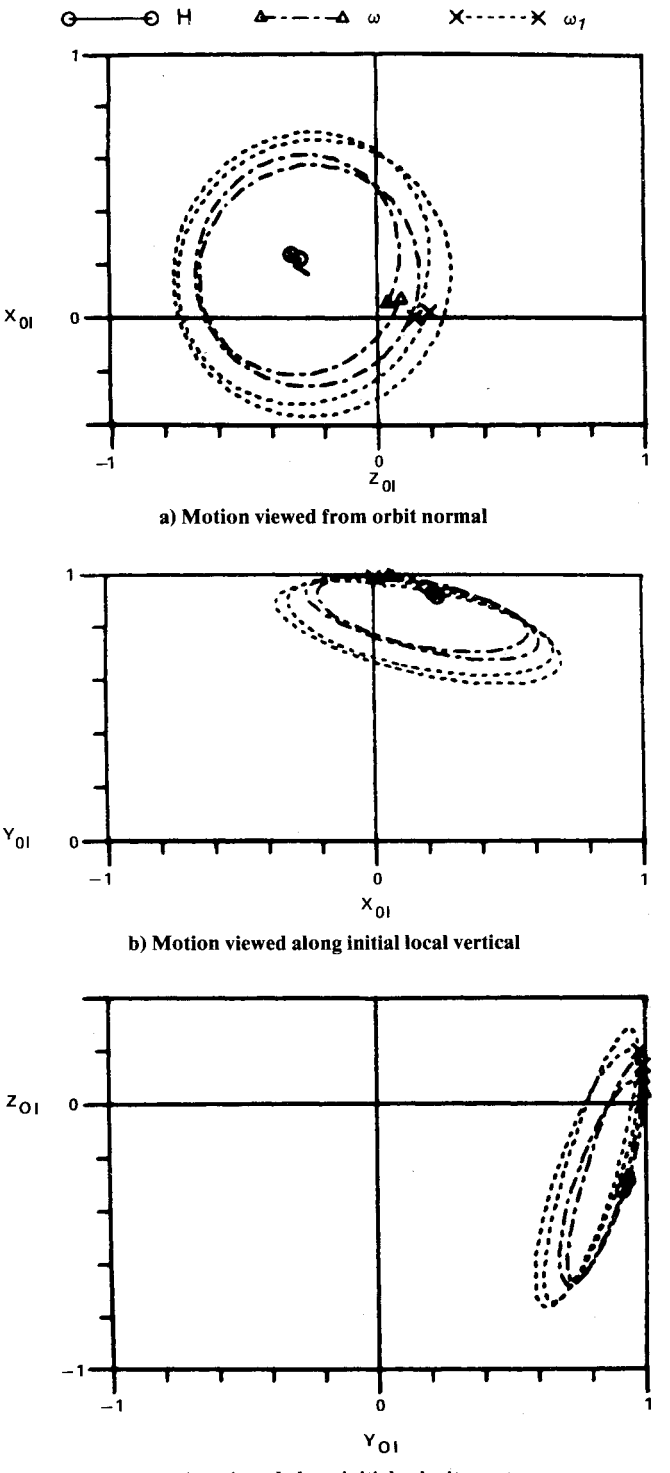


a) Motion viewed from orbit normal

b) Motion viewed along initial local vertical

c) Motion viewed along initial velocity vector

Fig. 5 Motion of the momentum vector, angular velocity vector, and spin axis in an inertially fixed system initially aligned with the orbital coordinate frame.

Occasionally the sun would pass within the field of view of the acquisition sun sensor. These were the only sources of information concerning the orientation of the body in space. Both the data from the simulation and the spacecraft indicated that while the vehicle was undergoing considerable motion and the pattern was rather complex, the motion was not random.

An example of the motion observed can be obtained by initializing the simulation program using data from the on-board rate gyros and sun sensors. These data were taken in March 1978 about 24 h prior to the activation of attitude

control. Initially the Skylab was oriented with the $x$ principal axis in the $y_0$-$z_0$ plane, approximately 8 deg off the orbit normal. The $z$ body axis was directed up, 2 deg off the radius vector in the $y_0$-$z_0$ plane. This resulted in a 15 deg angle between the solar panels and the sun line. The Skylab was spinning about the $x$ principal axis at a rate of 1.73 deg/s ($\omega_I$). The total angular rate about the $y$ and $z$ principal axes was 0.203 deg/s. Figure 4 shows the initial orientation of the vehicle, the angular momentum vector $H$, and the angular rate vector $\omega$ in the orbital coordinate system.

Since the external torques are small and the vehicle is approximately symmetrical about the $X_p$ axis, the motion over a short time period (15-30 min) can be compared to that of a torque-free spinning body of revolution.[16] If we consider the torque-free motion, the angular momentum would remain constant in magnitude, and its direction fixed in space. For the angular rates of 1.73 deg/s and 0.203 deg/s, the angle between $\omega_I$ and $H$ would remain constant at 31 deg. The angle between $H$ and the oribt normal would be a constant 24 deg. If viewed by a space-fixed observer, both $\omega$ and $\omega_I$ would precess about the angular momentum vector at a rate of 0.4 deg/s (15 min/cycle).

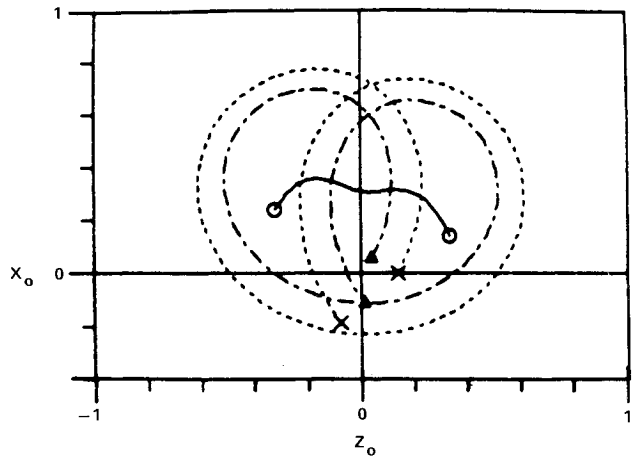


**a) Momentum vector, angular velocity vector, and spin axis projected on orbital plane**

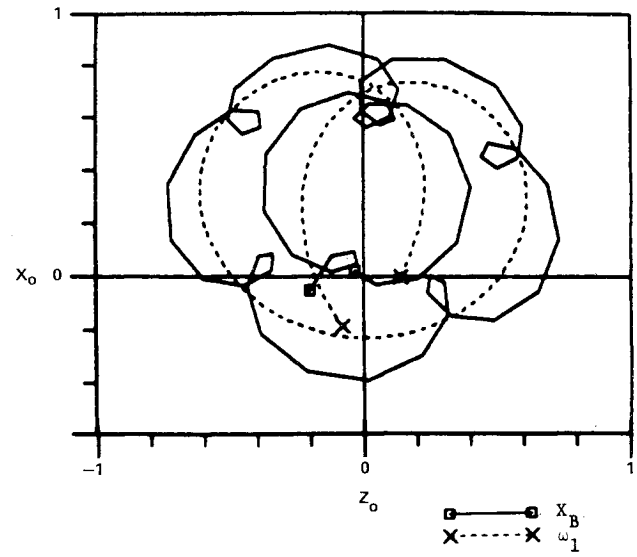


**b) Spin axis and $X$ vehicle axis projected on orbital plane**

**Fig. 6 Motion in a rotating orbital coordinate frame.**

Simulation results, which include both the effects of external torques and an asymmetric vehicle are shown in Fig. 5 for approximately 1/3 of an orbit (30 min). The OI coordinate system is inertially fixed and is initially aligned with the orbital coordinate frame O. A unit vector along the angular momentum is represented by a solid line and the symbol 0. The long-short dashed line with the symbol Δ represents a unit vector along $\omega$ and a short dashed line with the symbol $x$ represents a unit vector along the $X_p(\omega_I)$ axis. Figure 5a presents traces of these unit vectors in the orbital plane ($x_{0I}$ − $z_{0I}$) as viewed from the orbit normal. During this 30 min interval, the momentum vector remains nearly constant in this plane, while the $\omega$ and $\omega_I$ vectors complete a little more than two revolutions about $H$. Figures 5b and 5c show the same data in the $x_{0I}$-$y_{0I}$ plane and the $y_{0I}$-$z_{0I}$ plane, respectively, and show that the motion of these vectors is confined to one side of the orbit plane. For the torque-free symmetrical body motion, the momentum vector would appear as a single point, while the $\omega$ and $\omega_I$ vectors would trace repeating circles about that point.

In later 1977, when observations indicated the Skylab was no longer in the stable gravity gradient attitude, it was first thought to be tumbling in an unpredictable manner. At best, the ground observations could give the orientation of the longitudinal axis of the Skylab, and at times, the direction of the solar panels. Figure 6a is the motion of $H$, $\omega$, and $X_p$ in the orbit plane as they would appear in the rotating orbital coordinate system O. While the motion appears more complex when viewed in this system, there still exists a definite pattern. Because of the offset of the principal spin axis from the longitudinal body axis (≈ 10 deg), determining the motion of the Skylab based on ground observations was more difficult. Figure 6b shows again the motion of $X_p$ in the orbit plane as it would appear to a ground observer. In addition, the motion of the $x$ body axis is represented by the solid line with the symbol □. As the principal axis cones about the angular momentum vector at a rate of 0.4 deg/s, the body axis is rotating about the principal axis at a rate of 1.73 deg/s.

In view of the similarity between the numerical results and the torque-free solution, it seemed that the body rates measured by the on-board rate gyro system should also exhibit some consistency when viewed in the same way.

Table 2 presents measured rate data from the vehicle obtained in early March. As previously stated, the $x$ rate gyro was saturated and the roll rate determined from the solar arrays was 1.20 deg/s. This rate was assumed to be along the $X_p$ axis. The angle between $X_p$ and the angular velocity vector, $\theta$, and the angle between $X_p$ and the momentum

**Table 2 Skylab body rates measured 3/11/78**

| Time, h: min:s | Rate about $X_p$, deg/s | Rate about $Y_B$, deg/s | Rate about $Z_B$, deg/s | $\Phi$, deg | $\theta$, deg | $\dot{\psi}$, deg/s | $\dot{\nu}$, deg/s |
|---|---|---|---|---|---|---|---|
| 20:38:50 | 1.20 | +0.014 | +0.165 | 12.2 | 2.3 | 0.24 | 0.96 |
| 39:00 | ↓ | +0.009 | +0.166 | 12.3 | 2.3 | 0.24 | 0.96 |
| 39:20 | ↓ | −0.002 | +0.170 | 12.6 | 2.4 | 0.24 | 0.96 |
| 39:40 | ↓ | −0.010 | +0.178 | 12.3 | 2.3 | 0.24 | 0.96 |
| 40:00 | ↓ | −0.015 | +0.186 | 12.1 | 2.3 | 0.24 | 0.96 |
| 40:20 | ↓ | −0.012 | +0.198 | 10.3 | 1.9 | 0.24 | 0.96 |
| 40:40 | ↓ | −0.012 | +0.260 | 15.2 | 2.9 | 0.24 | 0.96 |

**Table 3 Trends derived from measured rates**

| Date | $\Phi$, deg | $\theta$, deg | $\dot{\psi}$, deg/s | $\dot{\nu}$, deg/s | Rate about $X_p$, deg/s |
|---|---|---|---|---|---|
| 3/11/78 | 12.4 | 2.3 | 0.24 | 0.96 | 1.20 |
| 5/5/78 | 22.8 | 4.7 | 0.34 | 1.28 | 1.60 |
| 5/7/78 | 23.9 | 5.0 | 0.35 | 1.28 | 1.60 |
| 5/10/78 | 21.2 | 4.3 | 0.34 | 1.28 | 1.60 |
| 5/30/78 | 28.1 | 5.9 | 0.39 | 1.41 | 1.76 |
| 6/01/78 | 27.0 | 5.7 | 0.39 | 1.41 | 1.76 |
| 6/06/78 | 36.0 | 8.1 | 0.42 | 1.39 | 1.73 |
| 6/07/78 | 31.0 | 6.7 | 0.40 | 1.39 | 1.73 |

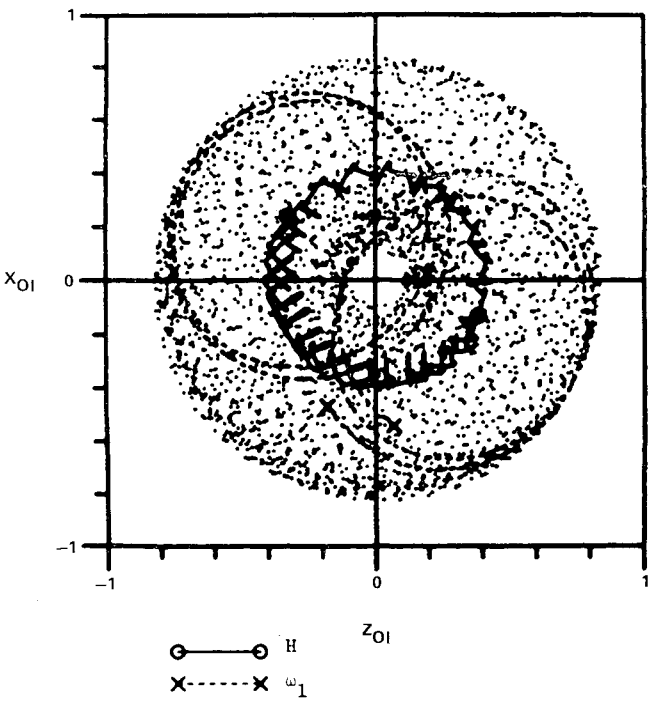


**Fig. 7 Motion of momentum vector and spin axis for 24 h period as viewed in an inertially fixed system.**

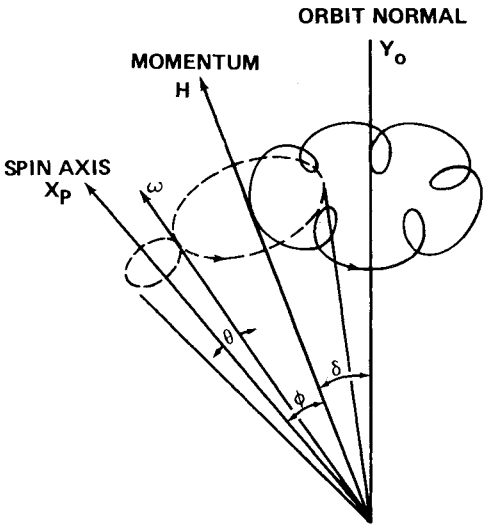


**Fig. 8 Motion of vehicle axis of symmetry $X_p$, angular velocity vector $\omega$, and momentum vector $H$, as viewed inertially.**

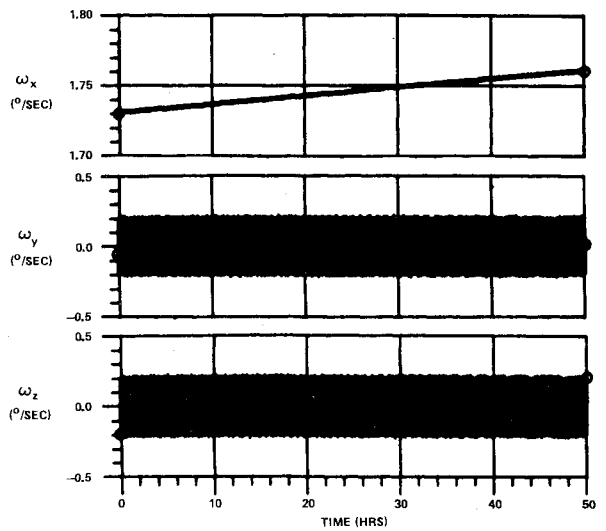


**Fig. 9 Body rates vs time.**

vector, $\phi$, were computed using the equations of Ref. 16. In the same fashion, the precession and nutation rates $\dot{\psi}$ and $\dot{\nu}$ were determined from the given rate data.

If the torque-free approximation were strictly true and if the measurements were free from error, all four of these parameters would have constant values. While this is not precisely correct, note the consistency that is introduced by viewing the data in this form as opposed to looking at the body rates themselves. Data taken on subsequent days also showed the same pattern and gave confidence that this approach was applicable. When the processed data from several days was examined some long-term trends were indicated (Table 3). These data represent all the measurements obtained from the vehicle rate gyro system between initial contact (3/6/78) and control moment gyro activation (6/9/78). These data show that over this period the spin rate increased with time, as did the precession and nutation rates. During the same time, the angle between the $x$ principal axis and the momentum vector grew from 12 to 30 deg giving a much wider cone.

While the torque-free approximation can be used for the short-term motion, the effect of the external torques must be considered for the long-term motion. These torques, though small, cause the momentum vector to precess about the orbit normal. For this case, the period of precession is approximately 14 h.

Simulation results covering 21 h are shown in Fig. 7. The solid line shows the motion of the angular momentum vector in the inertial system as viewed from the orbit normal. For clarity, the $x$ principal axis is represented by dots with its motion for a 30 min period at the beginning and ending of this time frame indicated by the dashed circles. A pictorial representation of this motion as it would appear to an inertially fixed observer is shown in Fig. 8.

While the cone angles and rates in late 1977 differ from the simulation results shown here, the basic motion of the Skylab was the same. Thus, it is easy to see that early ground observations, with sighting times of only a few minutes duration, might give the indication that the motion of the Skylab was unpredictable.

Shown in Fig. 9 are the angular rates about the principal axes. These simulation results show that while the rates about the $Y_p$ and $Z_p$ axes oscillate between $\pm 0.2$ deg/s, their average value remains constant. The rate about the $X_p$ axis has a small short-term oscillation with the average value increasing at a constant rate due to the aerodynamic torque. Figure 10 presents another comparison of measured data and simulation results. Just prior to activation of the attitude control system, a systematic effort was made to deduce the vehicle's attitude. This was important because the vehicle had to be maneuvered to face the sun and, as there was no on-

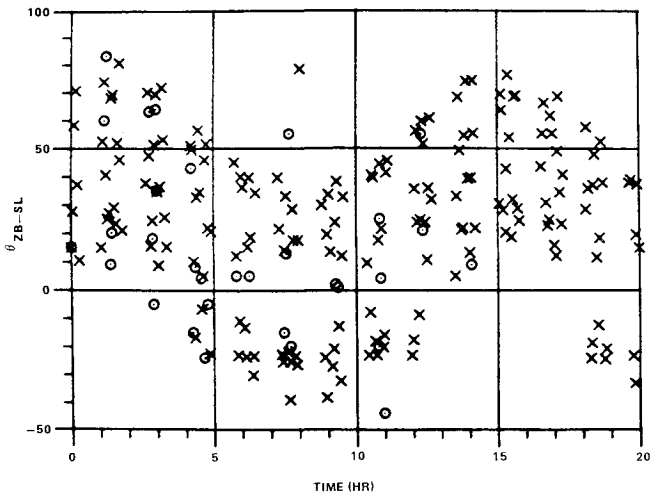


**Fig. 10 Comparison of measured vehicle attitude relative to solar vector with simulation results.**

board attitude reference, some idea as to where the vehicle was expected to be pointed at a given time was needed. The vehicle's solar array system was arranged so that the plane of the arrays was perpendicular to the vehicle's $Z_B$ axis. Since the vehicle was rotating at nearly 2 deg/s about the $X_p$ axis, the side of the arrays with the solar cells attached would go through a light-dark cycle every 3 min. From an examination of the maximum output level and knowledge of the array performance, one could estimate the minimum angle between the $Z_B$ axis and the sunline ($\theta_{ZB\text{-}SL}$). This would only give a magnitude, however, and other data had to be used to determine sign. Fortunately for most of this period, the acquisition sun sensor was available, and though the angles were usually beyond its linear range, its signature did indicate sign. The O points plotted in Fig. 10 are the result of combining these data to give the minimum angle between $Z_B$ and the sunline. Note, there are some data gaps. These were due to the necessity of having the vehicle simultaneously in the sun and over the ground station.

The $x$ points in Fig. 10 were obtained from the simulation and represent the vehicle's attitude to the solar vector in the manner indicated above. Since the flight data consist of discrete points covering quite a range, it would be incorrect to say that the simulation results duplicate the observed data in the usual sense. However, the simulation results and observed data do exhibit the same ranges and periodic characteristics leading one to conclude that the vehicle's motion was probably very close to that indicated by the simulation.

## Conclusions

The motion of Skylab prior to the resumption of active control provided an illustration of the effect of aerodynamic and gravity gradient torques on vehicle motion. Once the vehicle began to rotate, gyrodynamic effects began to play an important part and this became more pronounced as the spin rate increased. Though complex, this behavior can be predicted both numerically and analytically. In the course of this study, the complementary roles of both numerical integration and closed-form analysis were demonstrated. In cases such as this, a combined approach will produce better results than either approach alone.

In the future, retrieval of derelict spacecraft may be required for disposal or salvage and this will require some description of the expected behavior of such bodies. In the presence of even small aerodynamic torques, these vehicles will, generally, be unstable without appreciable energy dissipation. This implies a need for either supplying enough damping to insure eventual capture in a stable gravity gradient mode or the development of systems capable of capturing spacecraft undergoing large angular rotations, such as was experienced in this case.

## References

[1] Cobb, A.C., "Skylab Mission Final Mass Properties Report," NASA Memo S&E-ASTN-SA, March 5, 1974.

[2] Garber, T.B., "Influence of Constant Disturbing Torques on the Motion of Gravity-Gradient Stabilized Satellites," *AIAA Journal,* Vol. 1, April 1963, pp. 968-969.

[3] Nurre, G.S., "Effects of Aerodynamic Torque on an Asymmetric, Gravity-Stabilized Satellite," NASA TM X-53688, Jan. 2, 1968.

[4] Sperling, H.J., "Effect of Gravitational and Aerodynamic Torques on a Rigid Skylab-Type Satellite," NASA TM X-64865, June 1, 1974.

[5] Pack, H., "Vibration Data for the Skylab Cluster Less Command Service Module," NASA S&E-AERO-DD-8-71, Feb. 11, 1971.

[6] Gyrofl, R.A., "Orbital Aerodynamic Data for the Updated Skylab I In-Orbit Configuration," Northrop Services Memo M-9230-73-197, July 11, 1973.

[7] Pringle, R., "Bounds on the Librations of a Symmetrical Satellite," *AIAA Journal,* Vol. 2, 1964, pp. 908-912.

[8] Meirovitch, L. and Wallace, F.B., "On the Effect of Aerodynamic and Gravity Gradient Torques on the Attitude Stability of Satellites," *AIAA Journal,* Vol. 4, 1966, pp. 2196-2202.

[9] Cochran, J.E., "Effects of Gravity-Gradient Torque on the Rotational Motion of a Triaxial Satellite in a Precessing Elliptical Orbit," *Celestial Mechanics,* Vol. 6, 1972, pp. 126-150.

[10] Pringle, R., "Effect of Perturbed Orbital Motion on a Spinning Symmetrical Satellite," *Journal of Spacecraft and Rockets,* Vol. 11, 1974, pp. 451-455.

[11] Thomson, W.T., "Spin Stabilization of Attitude Against Gravity Torque," *Journal of Astronautical Science,* Vol. 9, 1962, pp. 31-33.

[12] Auelmann, R.R., "Regions of Libration for a Symmetrical Satellite," *AIAA Journal,* Vol. 1, 1963, pp. 1445-1447.

[13] Likins, P.W., "Stability of a Symmetrical Satellite in Attitudes Fixed in an Orbiting Reference Frame," *Journal of Astronautical Sciences,* Vol. XII, 1965, pp. 18-24.

[14] Beletskii, V.N., "Motion of an Artificial Satellite About Its Center of Mass," NASA TT F-425, 1966.

[15] NASA Space Vehicle Design Criteria (1973): Models of Earth's Atmosphere (90 to 2500 km), NASA SP-8021.

[16] Greenwood, D.T., *Principles of Dynamics,* Prentice Hall, Inc., Englewood Cliffs, N.J., 1965, Chap. 8.

[17] Kane, T.R., Marsh, E.L., and Wilson, W.G., Letter to Editor, *Journal of Astronautical Science,* Vol. 9, 1962, pp. 108-109.